JACS
JOURNAL OF THE AMERICAN CHEMICAL SOCIETY

Communication

pubs.acs.org/JACS

Hydrogen-Bonding Partner of the Proton-Conducting Histidine in the Influenza M2 Proton Channel Revealed From ^{1}H Chemical Shifts

Mei Hong,* Keith J. Fritzsching,‡ and Jonathan K. Williams‡

Department of Chemistry, Iowa State University, Ames, Iowa 50011, United States

Supporting Information

ABSTRACT: The influenza M2 protein conducts protons through a critical histidine (His) residue, His37. Whether His37 only interacts with water to relay protons into the virion or whether a low-barrier hydrogen bond (LBHB) also exists between the histidines to stabilize charges before proton conduction is actively debated. To address this question, we have measured the imidazole $^{1}H^{N}$ chemical shifts of His37 at different temperatures and pH using 2D $^{15}N-^{1}H$ correlation solid-state NMR. At low temperature, the H^{N} chemical shifts are 8−15 ppm at all pH values, indicating that the His37 side chain forms conventional hydrogen bonds (H-bonds) instead of LBHBs. At ambient temperature, the dynamically averaged H^{N} chemical shifts are 4.8 ppm, indicating that the H-bonding partner of the imidazole is water instead of another histidine in the tetrameric channel. These data show that His37 forms H-bonds only to water, with regular strength, thus supporting the His−water proton exchange model and ruling out the low-barrier H-bonded dimer model.

The influenza M2 protein forms a tetrameric proton channel important for the virus lifecycle.[1−3] Activated by the low pH environment of the endosome, the channel opens to acidify the virion, which causes viral uncoating. The mechanism of proton conduction through M2 has long been debated. Early computational studies and functional data diverged on whether proton conduction occurs by Grotthuss hopping along a water wire[4,5] or requires conformational changes of the only titratable residue in the transmembrane (TM) domain, His37[6] (Figure 1a). Recent data have ruled out the water wire model and converged on the active participation of His37 in proton relay. Evidence for proton shuttling by His37 came from magic angle spinning (MAS) ^{15}N NMR spectra showing chemical exchange of the imidazole nitrogens between the protonated (NH) and unprotonated (N) states at the physiological pH of the endosome.[7] This exchange is accompanied by low-pH specific imidazolium reorientation on the microsecond time scale with an energy barrier comparable to the proton conduction barrier.[8]

Despite the general consensus that His37 shuttles protons, the mechanism by which charge is stabilized in the His37 tetrad is still actively debated. The ^{15}N chemical exchange and imidazolium reorientation led to the proposal that His37−water H-bonding and proton exchange are sufficient for proton conduction (Figure 1b)[7] and that excess protons are stabilized by delocalization over the His37 tetrad and the surrounding water molecules.[9] In contrast, an alternative model posits a LBHB between a neutral and a cationic histidine in the +2 state of the channel (Figure 1c),[10] which stabilizes the charges before channel activation. This model was motivated by the observation of a very high pK_a of 8.2 for the first two protonation steps in DMPC/DMPG bilayer-bound M2 TM peptide (M2TM),[10] and by computational modeling of the His37 side-chain structure.[11] The latter yielded His37 (χ_1, χ_2) torsion angles of (180°, 90°) to establish the putative Nε2−H···Nδ1 H-bond. Recently reported chemical shift multiplicity of some of the TM residues,[12,13] although observed at neutral pH, was also interpreted as supporting the LBHB model.

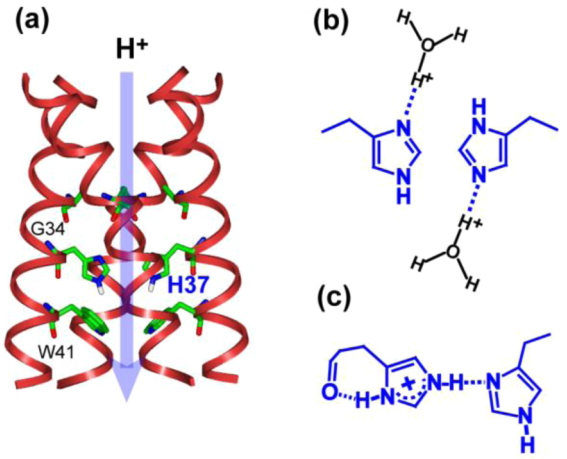

Figure 1. Two proton conduction models for the influenza M2 channel. (a) Structure of M2TM at pH 6.5 (PDB: 3LBW), showing the location of the key His37 and Trp41. (b) His37−water proton exchange model. (c) His−His low-barrier H-bonded dimer model. The dimer of dimer state is proposed to exist stably in the +2 tetrad to stabilize charge before proton transfer to water.

Equilibrium conformation of His37 measured by solid-state NMR[8] and X-ray crystallography[9,14] at acidic pH have so far shown no direct His−His H-bonding: the His37 χ_1 and χ_2 angles were measured to be ∼180° in both lipid bilayers and detergents, which points the Nε2-H and Nδ1 toward the interior and exterior of the channel rather than toward each other. $^{13}C-^{13}C$ 2D correlation spectra of the +2 charged channel displayed no imidazole−imidazolium cross peaks,[7] also challenging the LBHB model. However, the ^{15}N NMR spectra

Received: July 28, 2012
Published: August 29, 2012

   dx.doi.org/10.1021/ja307453v | J. Am. Chem. Soc. 2012, 134, 14753−14755

showing $N \leftrightarrow NH$ chemical exchange, can, in principle, be due to either His−water proton transfer or His−His H-bonding. Thus, we sought more definitive evidence for the H-bonding partner of His37 as well as the strength of the His37 H-bond. The strength of H-bonds can be discerned through the ^{1}H chemical shift: a proton in a low-barrier or strong H-bond should have a large chemical shift of greater than 16 ppm,[15−18] whereas a proton in a regular unequal-well H-bond should have a smaller chemical shift of 8−15 ppm.[19,20] The identity of the H-bonding partner for membrane proteins in hydrated lipid bilayers can be determined through the temperature dependence of the ^{1}H chemical shift. Between −30 °C and +30 °C, the diffusion rates of water in the channel change significantly;[21,22] thus, a regular N−H···O H-bond should involve only one or few water molecules at low temperature but should undergo rapid exchange with many water molecules at physiological temperature. This should result in a ^{1}H chemical shift close to the imidazole H^N value at low temperature but a population-weighted value near the water ^{1}H chemical shift at high temperature. In contrast, for a pK_a-matched N−H···N LBHB,[23,24] the central proton has a much higher activation energy for exchange with water;[25] moreover proton transfer dynamics between the two nitrogens is ultrafast. Thus, the ^{1}H chemical shift will be insensitive to temperature at this range and remain large. Thus, the low-temperature ^{1}H chemical shift reveals the H-bond strength, whereas the high-temperature chemical shift indicates the identity of the H-bonding partner.

We measured the ^{1}H chemical shift using the 2D ^{15}N−^{1}H heteronuclear correlation (HETCOR) experiment. To detect only cross peaks due to direct N−H dipolar coupling without relayed transfer, we suppressed ^{1}H spin diffusion using ^{1}H homonuclear decoupling during the evolution period and the ^{1}H−^{15}N cross-polarization period.[26] His37-labeled M2TM bound to a virus-mimetic lipid membrane were measured at pH 6.0, 4.5, and 8.5.[8] Since all initial experiments that led to the LBHB model were conducted on M2TM, we used the same construct to avoid potential ambiguities in interpretation. Previous measurement of His37 pK_a's in this virus-mimetic membrane indicated that the channel was 80% in the +2 state at pH 6, in a mixed +3 and +4 state at pH 4.5, and about 90% neutral at pH 8.5.[7] Thus, the pH 6.0 sample is the closest to the putative LBHB state. The 2D HETCOR spectra were measured at 245 K to determine the H-bond strength and 296 K to determine the H-bonding partner.

Figure 2a shows the 2D HETCOR spectra of the pH 6.0 sample. At 245 K, the imidazole Nε2 (τ tautomer) and Nδ1 (π tautomer) peaks at 160−180 ppm exhibit ^{1}H chemical shifts of 8−12 ppm, similar to the backbone amide ^{1}H chemical shift range. Thus, imidazole H^N lies in a regular H-bond. For comparison, histidine hydrochloride (Figure S1, Supporting Information [SI]) shows a large Hδ1 chemical shift of 16.8 ppm due to a strong intermolecular H-bond to a C═O with an N···O distance of 2.63 Å.[27] Both ^{15}N and ^{1}H shifts reflect the strength of the H-bond: small ^{15}N and ^{1}H shifts indicate a stronger covalent N−H bond, while large shifts indicate a more deprotonated nitrogen or a stronger H-bond.[17,18] The correlation gives a slope of ∼3 between the ^{15}N and ^{1}H chemical shifts (Figure 2a). The ^{1}H shift distribution (Figure S2, SI), detected for both backbone and imidazole nitrogens, indicates a distribution of H-bond strengths. The backbone distribution is likely due to varying degrees of helix ideality in an ensemble with mixed protonation states, while the imidazole H^N shift distribution can be attributed to the presence of

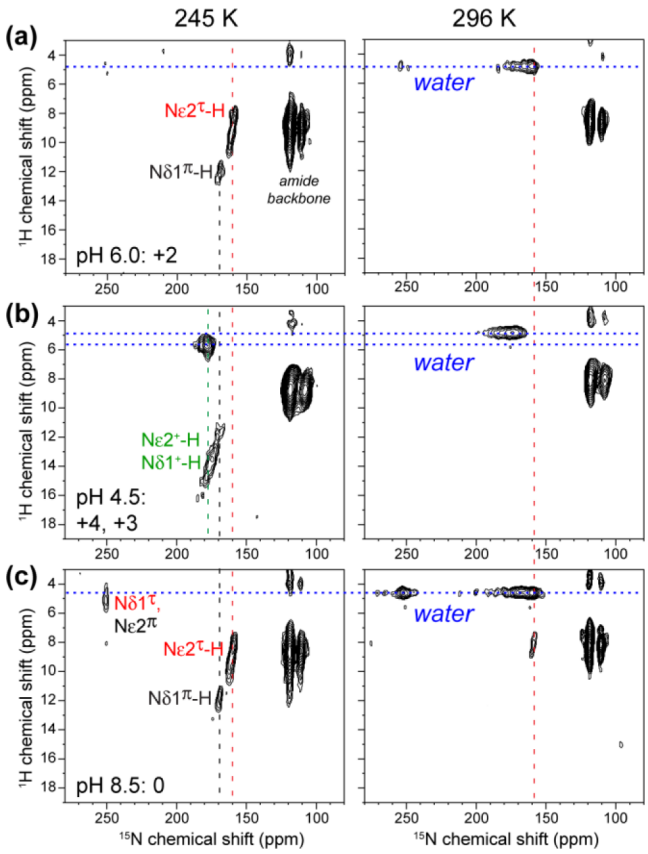

Figure 2. Two-dimensional ^{15}N−^{1}H HETCOR spectra of membrane-bound His37-labeled M2TM at (a) pH 6.0, (b) pH 4.5, and (c) pH 8.5 at 245 K (left) and 296 K (right). The main charged states of the M2TM channel at each pH are indicated. The ^{1}H dimension of the spectrum was measured with ^{1}H homonuclear decoupling to eliminate spin diffusion effects. Assignments are shown in red for the neutral τ tautomer, black for the neutral π tautomer, and green for cationic His37.

multiple N−H species, including Nε2H(τ), Nδ1H(π), and the Nε2H and Nδ1H of cationic imidazolium (Figure S3, SI).

When the temperature increased to 296 K, the imidazole ^{1}H chemical shifts decreased uniformly to 4.8 ppm, indicating definitively that the H-bonding partner of His37 is water instead of another His. Since ^{1}H homonuclear decoupling was applied in the experiment, both rigid and mobile protons were equally detected; thus, the observed ^{1}H chemical shift near the unperturbed water frequency indicates a large number of water molecules in exchange with the imidazole nitrogens. For comparison, the backbone H^N chemical shift is unaffected by temperature, as expected for the persistence of N−H···O═C H-bonds at these temperatures.

The 2D spectra of the pH 4.5 sample (Figure 2b) further support the His37−water interaction model.[7,9] Even at low temperature, the 178 ppm ^{15}N peak already shows a water ^{1}H cross peak (5.7 ppm) in addition to the Hε2/Hδ1 signal (12−15 ppm), consistent with previous data showing a more hydrated channel at this low pH.[28] The Hε2/Hδ1 chemical shift is larger than at pH 6, indicating stronger H-bonds. This is consistent with the previously measured N−H bond elongation at this pH.[8] The ^{15}N/^{1}H chemical shift slope is the same as at pH 6.0 (Figure S4, SI), as expected for the intrinsic correlation between ^{15}N protonation and N−H···O H-bond strength. Again, the identity of the H-bonding partner is determined by

dx.doi.org/10.1021/ja307453v | J. Am. Chem. Soc. 2012, 134, 14753−14755

the high-temperature spectrum, which shows a ^{1}H chemical shift at the water position of 4.8 ppm, indicating that His37 H-bonds only to water.

At pH 8.5, the high-temperature spectrum retained the dominant water cross peak, but a weak signal at ∼8 ppm was also detected and can be assigned to Hε2. Although the channel does not conduct protons at this pH, some water molecules are still present, for example between His37 and Trp41,[8,9,29] thus allowing polarization transfer to ^{15}N. At low temperature, the unprotonated nitrogen, mainly Nδ1, exhibits a ^{1}H cross peak at ∼5 ppm due to Hε1, as verified by the spectrum of amino acid histidine (Figure S1, SI).[27]

These low-temperature ^{1}H chemical shifts are smaller than expected for an LBHB or a strong H-bond, while the high-temperature ^{1}H chemical shifts reveal the H-bonding partner to be water. Thus, the data support the direct His37−water interaction model and rule out the His−His LBHB-dimer model. The 1.65 Å crystal structure at pH 6.5[9] detected tightly clustered water molecules near the His37 tetrad, with N···O distances as short as 2.8 Å, also supporting direct His37−water interactions. On the other hand, all experimental data so far, including the initial ^{15}N NMR spectra from which the dimer model was proposed,[10] show an *absence* of imidazole−imidazolium H-bond. An LBHB entails either a single ^{15}N peak at the averaged chemical shift between N and NH for equal-well potentials or two ^{15}N peaks centered around the averaged frequency for unequal-well potentials. Instead, the ^{15}N spectra showed a single peak away from the averaged chemical shift, without the partner peak. Molecular modeling of the HxxxW structure[11] was questionable because it used the putative LBHB as a starting distance restraint to enforce the expected geometry during MD simulations. Finally, the LBHB model implies a hydrophobic environment for the donor and acceptor with a very small pK_a difference,[30] which contradicts the observed different proton affinities of Nε2 and Nδ1 in His37 and the high hydration of this residue.

In conclusion, temperature-dependent ^{1}H chemical shifts of the His37 side chain indicate that His37−water H-bonding and proton exchange dominate the equilibrium structure of the His37 tetrad throughout the whole pH range. His−His interactions are indirectly mediated by water. If a direct His−His H-bond is too transient to be detectable by NMR, then it cannot be an LBHB and cannot provide stabilization for the dimer state. We propose that charges are stabilized by water-mediated interactions[7,9] and by cation−π interaction between His37 and Trp41.[5]

This temperature-dependent ^{1}H chemical shift approach avoids the difficulty of measuring N···N and N···O distances across a H-bond by NMR; moreover, it directly reveals the structure of the most essential player in a proton relay chain. It is applicable to both biological and synthetic proton conductors to understand the nature of the H-bond in proton transport.

■ ASSOCIATED CONTENT

Supporting Information

Experimental procedures and additional spectra. This material is available free of charge via the Internet at http://pubs.acs.org.

■ AUTHOR INFORMATION

Corresponding Author

mhong@iastate.edu

Author Contributions

‡These authors contributed equally.

Notes

The authors declare no competing financial interest.

■ ACKNOWLEDGMENTS

We thank Professor Schmidt-Rohr for useful discussions. This work is supported by NIH Grant GM088204.

■ REFERENCES

(1) Pinto, L. H.; Lamb, R. A. *J. Biol. Chem.* **2006**, *281*, 8997−9000.
(2) Cady, S. D.; Luo, W. B.; Hu, F.; Hong, M. *Biochemistry* **2009**, *48*, 7356−7364.
(3) Wang, J.; Qiu, J. X.; Soto, C. S.; DeGrado, W. F. *Curr. Opin. Struct. Biol.* **2011**, *21*, 68−80.
(4) Sansom, M. S. P.; Kerr, I. D.; Smith, G. R.; Son, H. S. *Virology* **1997**, *233*, 163−173.
(5) Okada, A.; Miura, T.; Takeuchi, H. *Biochemistry* **2001**, *40*, 6053−6060.
(6) Pinto, L. H.; Dieckmann, G. R.; Gandhi, C. S.; Papworth, C. G.; Braman, J.; Shaughnessy, M. A.; Lear, J. D.; Lamb, R. A.; DeGrado, W. F. *Proc. Natl. Acad. Sci. U.S.A.* **1997**, *94*, 11301−11306.
(7) Hu, F.; Schmidt-Rohr, K.; Hong, M. *J. Am. Chem. Soc.* **2012**, *134*, 3703−3713.
(8) Hu, F.; Luo, W.; Hong, M. *Science* **2010**, *330*, 505−508.
(9) Acharya, A.; Carnevale, V.; Fiorin, G.; Levine, B. G.; Polishchuk, A.; Balannick, V.; Samish, I.; Lamb, R. A.; Pinto, L. H.; DeGrado, W. F.; Klein, M. L. *Proc. Natl. Acad. Sci. U.S.A.* **2010**, *107*, 15075−15080.
(10) Hu, J.; Fu, R.; Nishimura, K.; Zhang, L.; Zhou, H. X.; Busath, D. D.; Vijayvergiya, V.; Cross, T. A. *Proc. Natl. Acad. Sci. U.S.A.* **2006**, *103*, 6865−6870.
(11) Sharma, M.; Yi, M.; Dong, H.; Qin, H.; Peterson, E.; Busath, D.; Zhou, H. X.; Cross, T. A. *Science* **2010**, *330*, 509−512.
(12) Andreas, L. B.; Eddy, M. T.; Chou, J. J.; Griffin, R. G. *J. Am. Chem. Soc.* **2012**, *134*, 7215−7218.
(13) Can, T. V.; Sharma, M.; Hung, I.; Gor'kov, P. L.; Brey, W. W.; Cross, T. A. *J. Am. Chem. Soc.* **2012**, *134*, 9022−9025.
(14) Stouffer, A. L.; Acharya, R.; Salom, D.; Levine, A. S.; Di Costanzo, L.; Soto, C. S.; Tereshko, V.; Nanda, V.; Stayrook, S.; DeGrado, W. F. *Nature* **2008**, *451*, 596−599.
(15) Brown, S. P. *Solid State Nucl. Magn. Reson.* **2012**, *41*, 1−27.
(16) Gilli, P.; Bertolasi, V.; Ferretti, V.; Gilli, G. *J. Am. Chem. Soc.* **2000**, *122*, 10405−10417.
(17) Lorente, P.; Shenderovich, I. G.; Golubev, N. S.; Denisov, G. S.; Buntkowsky, G.; Limbach, H. H. *Magn. Reson. Chem.* **2001**, *39*, S18−S29.
(18) Sharif, S.; Schagen, D.; Toney, M. D.; Limbach, H. H. *J. Am. Chem. Soc.* **2007**, *129*, 4440−4455.
(19) Berglund, B.; Vaughan, R. W. *J. Chem. Phys.* **1980**, *73*, 2037−2043.
(20) Barfield, M. *J. Am. Chem. Soc.* **2002**, *124*, 4158−4168.
(21) Nicotera, I.; Coppola, L.; Rossi, C. O.; Youssry, M.; Ranieri, G. A. *J. Phys. Chem. B* **2009**, *113*, 13935−13941.
(22) Takahara, S.; Nakano, M.; Kittaka, S.; Kuroda, Y.; Mori, T.; Hamano, H.; Yamaguchi, T. *J. Phys. Chem. B* **1999**, *103*, 5814−5819.
(23) Song, X. J.; McDermott, A. E. *Magn. Reson. Chem.* **2001**, *39*, S37−S43.
(24) Wehrle, B.; Zimmermann, H.; Limbach, H. H. *J. Am. Chem. Soc.* **1988**, *110*, 7014−7024.
(25) Lin, J.; Westler, W. M.; Cleland, W. W.; Markley, J. L.; Frey, P. A. *Proc. Natl. Acad. Sci. U.S.A.* **1998**, *95*, 14664−14668.
(26) Hong, M.; Yao, X. L.; Jakes, K.; Huster, D. *J. Phys. Chem. B* **2002**, *106*, 7355−7364.
(27) Li, S.; Hong, M. *J. Am. Chem. Soc.* **2011**, *133*, 1534−1544.
(28) Luo, W.; Hong, M. *J. Am. Chem. Soc.* **2010**, *132*, 2378−2384.
(29) Su, Y.; Hu, F.; Hong, M. *J. Am. Chem. Soc.* **2012**, *134*, 8693−8702.
(30) Schutz, C. N.; Warshel, A. *Proteins* **2004**, *55*, 711−723.

Supporting Information

Hydrogen Bonding Partner of the Proton-Conducting Histidine in the Influenza M2 Proton Channel Revealed From ^{1}H Chemical Shifts

Mei Hong*, Keith J. Fritzsching‡ and Jonathan K. Williams‡
Department of Chemistry, Iowa State University, Ames, Iowa 50011

NMR samples

The M2TM membrane samples were prepared as described before [1,2]. Briefly, Gly34, His37 and Ile39 or Ile42 labeled M2(22-46) were synthesized and purified using Fmoc solid-phase protocols by PrimmBiotech, and incorporated into a virus-mimetic membrane using detergent dialysis. The membrane consists of DPPC : DPPE : sphingomyelin : cholesterol (21 : 21 : 28 : 30 mole ratio). The detergent octyl-β-D-glucoside was used for solubilizing and reconstituting the peptide into the lipid membrane. The peptide : lipid molar ratio was 1 : 15. Hydrated membrane pellets were obtained by ultracentrifugation and packed into 4 mm MAS rotors for solid-state NMR experiments. Three M2TM samples at pH 6.0, 4.5 and 8.5 were measured, and histidine amino acid recrystallized at the same pH values served as control samples [3].

Solid-state NMR experiments

Solid-state NMR experiments were carried out on a Bruker AVANCE 600 MHz (14.1 Tesla) spectrometer using a 4 mm MAS probe. Typical radiofrequency (rf) field strengths were 40 kHz for ^{15}N and 80 kHz for ^{1}H. ^{15}N chemical shifts were referenced to the N-acetyl-valine signal at 122.0 ppm on the liquid ammonia scale. ^{1}H chemical shifts were calibrated indirectly to those of formyl-Met-Leu-Phe [4] and verified with the published ^{1}H chemical shifts of amino acid histidine at various pH [3]. 2D ^{15}N-^{1}H HETCOR spectra were measured at 245 K and 296 K under 10 kHz MAS. Lee-Goldburg (LG) cross polarization (CP) was used to remove ^{1}H spin diffusion during CP. The ^{1}H and ^{15}N power levels for LG-CP were optimized similarly to the histidine amino acids to ensure proper detection of the unprotonated ^{15}N signal. The LG-CP contact time ranged from 0.5 ms to 2 ms and the ^{1}H effective spin-lock field strength was 50 kHz. Longer contact time was avoided to minimize long-range ^{1}H-^{15}N correlation signals. During the ^{1}H evolution period (t_1), the FSLG [5] pulses for ^{1}H homonuclear decoupling used a transverse field strength of 80 kHz and a corresponding frequency jump of ±56.6 kHz. The FSLG-scaled effective t_1 dwell time was 47.15 μs, and the typical number of t_1 slices was 80 or 88, resulting in a maximum t_1 evolution time of ~2 ms. Several experiments were co-added for each final spectrum, and the total number of scans ranged from 512 to 1956 per spectrum.

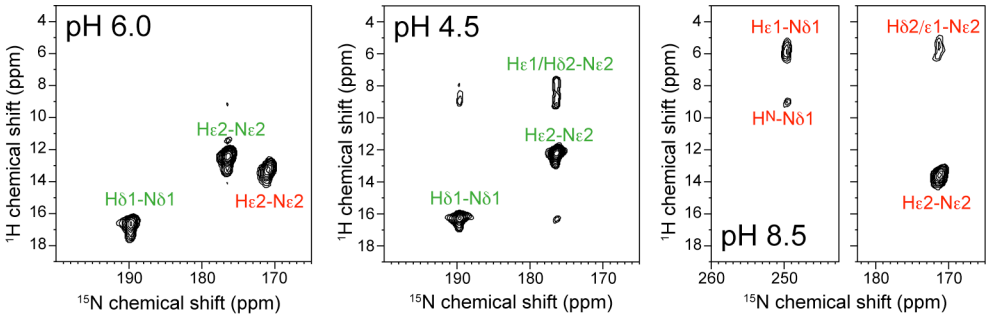

Figure S1. 2D ^{15}N-^{1}H HETCOR spectra of amino acid histidine at pH 6.0, 4.5 and 8.5. Assignments were made based on previous work [3]. These spectra were measured under the same FSLG and LG-CP conditions as the membrane-bound M2TM samples and served as controls for the ^{1}H chemical shifts. Note the downfield Hδ1 chemical shift of 17 ppm for cationic histidine (assigned in green) in the pH 4.5 and 6.0 spectra, which results from an intermolecular hydrogen bond with a backbone C=O with an R_{NO} of 2.63 Å [3]. Assignments for the neutral τ tautomer are given in red.

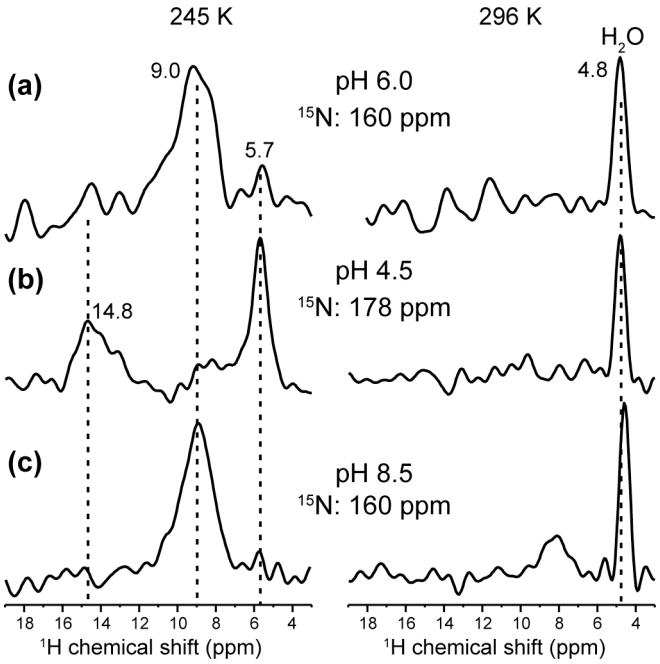

Figure S2. Representative ^{1}H cross sections from the 2D HETCOR spectra of membrane-bound M2TM at (a) pH 6.0, (b) pH 4.5, and (c) pH 8.5. Left and right columns are cross sections extracted from the 245 K and 296 K spectra, respectively.

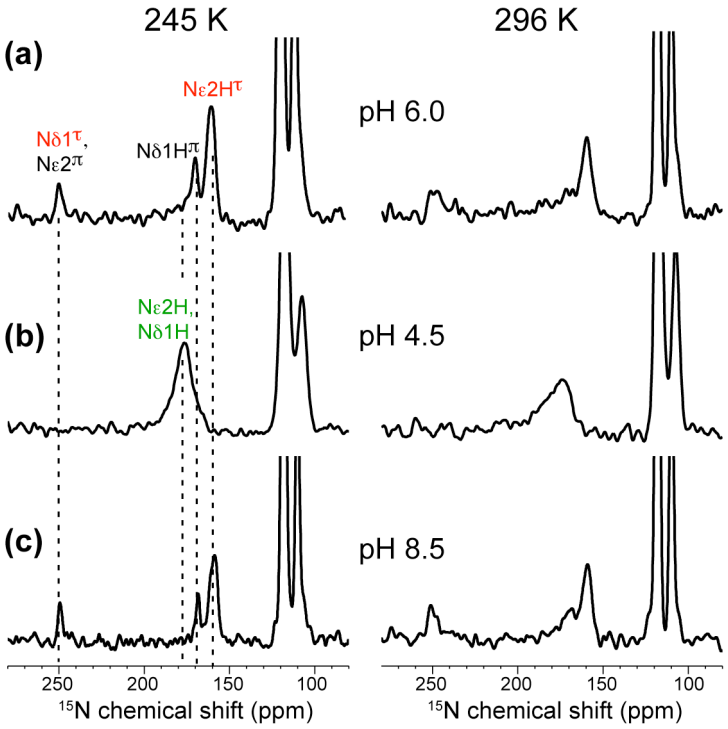

Figure S3. ^{15}N 1D LG-CP spectra of membrane-bound M2TM at 245 K (left column) and 296 K (right column) at pH 6.0 (a), pH 4.5 (b), and pH 8.5 (c). The spectra were measured immediately before and after the 2D HETCOR spectra under the same LG-CP conditions. ^{15}N assignments were based on previously reported 2D correlation spectra [1]. LG-CP contact time varied from 0.5 to 2 ms, which were shorter than necessary to reach equilibrium intensities for the unprotonated ^{15}N signal at 250 ppm, thus the spectral intensities shown here are not quantitative. Previous quantification of the ^{15}N CP-MAS spectra [2] showed that the relative intensity of the 250-ppm peak was about 2-fold higher at pH 8.5 than at pH 6 at 243 K.

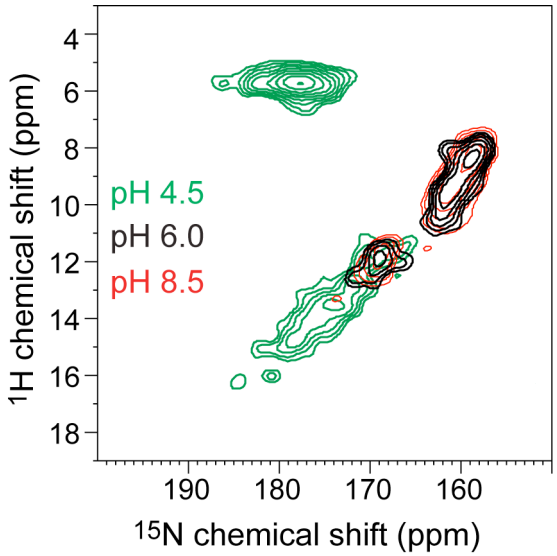

Figure S4. Superposition of the protonated imidazole ^{15}N region of the 245 K HETCOR spectra of membrane-bound M2TM at three pH values. The pH 4.5 sample shows larger ^{15}N and ^{1}H chemical shifts than the pH 6.0 and pH 8.5 samples due to stronger imidazolium-water H-bonding. In addition, a water cross peak is observed at pH 4.5 even at low temperature, consistent with the fact that the lowest-pH channel has the most hydrated pore [6]. The water ^{1}H chemical shift (~6 ppm) is larger at low temperature than at ambient temperature (~5 ppm) due to stronger H-bonding.

References

(1) Hu, F.; Luo, W.; Hong, M. *Science* **2010**, *330*, 505-508.
(2) Hu, F.; Schmidt-Rohr, K.; Hong, M. *J. Am. Chem. Soc,* **2012**, *134*, 3703-3713.
(3) Li, S.; Hong, M. *J. Am. Chem. Soc*. **2011**, *133*, 1534-1544.
(4) Rienstra, C. M.; Tucker-Kellogg, L.; Jaroniec, C. P.; Hohwy, M.; Reif, B.; McMahon, M. T.; Tidor, B.; Lozano-Perez, T.; Griffin, R. G. *Proc. Natl. Acad. Sci. USA* **2002**, *99*, 10260-10265.
(5) Bielecki, A.; Kolbert, A. C.; Levitt, M. H. *Chem. Phys. Lett*. **1989**, *155*, 341-346.
(6) Luo, W.; Hong, M. *J. Am. Chem. Soc*. **2010**, *132*, 2378-2384.